INTERNATIONAL JOURNAL FOR NUMERICAL AND ANALYTICAL METHODS IN GEOMECHANICS, VOL. 22, 303–322 (1998)

NUMERICAL ANALYSIS OF SOIL PLUG BEHAVIOUR INSIDE OPEN-ENDED PILES DURING DRIVING

D. S. LIYANAPATHIRANA, A. J. DEEKS AND M. F. RANDOLPH

Department of Civil Engineering, The University of Western Australia, Nedlands, 6907, Australia

SUMMARY

The plugging mechanism of infinitely-long open-ended piles is examined using numerical simulation of the wave propagation inside the soil plug and pile. It is shown that the key parameters for the plugging mechanism are the pile radius, the shape of the impact load, the shear wave velocity of the soil inside the pile, and the friction at the pile–soil interface. Consequently, the tendency of the pile to plug during driving can be assessed prior to the driving process by consideration of these key parameters. Existing one-dimensional models for the shaft response of open-ended piles are discussed and an improved model is presented. The differences between using one-dimensional models and finite element models to simulate the plugging process are examined. The differences are found to vary with the key parameters. Pile-in-pile and lumped-mass one-dimensional models are found to give satisfactory performance for some parameter combinations, while for others an axisymmetric finite element model must be used. © 1998 John Wiley & Sons, Ltd.

Int. J. Numer. Anal. Meth. Geomech., Vol. 22, 303–322 (1998)

Key words: pile driving; open-ended piles; plugging mechanism; one-dimensional modelling; stress wave propagation; finite element analysis

INTRODUCTION

Open-ended piles are widely used in construction, particularly for offshore foundations. When these piles are driven into the soil, a soil column is created inside the pile. The movement of this soil column with respect to the pile penetration reflects the mode of pile penetration in the soil (plugged, partially plugged or unplugged). This influences the pile–soil interaction during and after driving.

To obtain an effective model for the driving process, an accurate simulation of the wave propagation in the soil plug, pile and external soil is essential when the pile is subjected to an impact load. A number of researchers[1–4] have used the finite element method to achieve this goal. However, their results have been obtained using coarse finite element meshes, and no examination has been made of the shape of waves propagating in soil and pile. Moreover, all studies have used a single rectangular soil element with eight nodes across the soil plug, which cannot accurately simulate the propagation of a radial shear wave.

Although the finite element method can give accurate results if a sufficiently fine mesh is used, time integration of the finite element equations is time consuming. Therefore, it is useful to find

Corresponding to: M. F. Randolph, Department of Civil Engineering, The University of Western Australia, Nedlands, 6907, Australia

CCC 0363–9061/040303–20$17.50

Received 6 May 1996
Revised 23 July 1997

a simplified model to accurately simulate the pile driving process, and to identify the factors affecting the mode of pile penetration. As a first step towards obtaining such a model, this paper examines the behaviour of an open-ended pile to impact loading, neglecting end effects.

The paper commences with a dimensional analysis of the driving of open-ended piles. Then a detailed study of elastic and inelastic wave propagation inside the soil plug, carried out using the finite element method, is reported. The purpose of this study is to understand the wave propagation inside the soil plug, the fineness of the mesh required, and the factors affecting the penetration mode of the pile. Finally, the finite element results are compared with results obtained from simplified one-dimensional pile-in-pile and lumped-mass models.

NUMERICAL MODEL

An axisymmetric finite element model is used in this analysis. Since the end effects are not taken into account, soil at the pile toe level (inside and outside the pile) is truncated by applying a standard viscous boundary and the pile is truncated similarly by applying a dashpot equivalent to the impedance of the pile. This one-dimensional viscous boundary absorbs the waves travelling in the downward direction, simulating the infinitely-long condition. The soil field surrounding the pile shaft is truncated by the use of plain strain boundary equations developed by Deeks and Randolph[5] for axisymmetric shear and dilation waves, as shown in Figure 1.

The force exerted on top of the pile by the falling hammer is modelled using the ram-cushion-anvil model developed by Deeks and Randolph.[6]

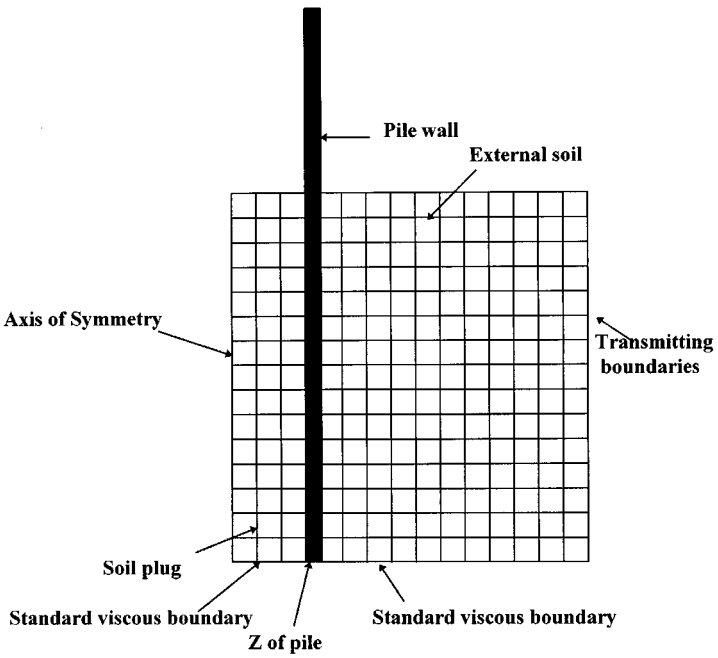

Figure 1. Finite element model used for the analysis

In the finite element model, the pile is modelled using three-node tube elements with vertical and radial degrees of freedom, but neglecting radial inertia. Soil is modelled using eight-node rectangular elements with four-point Gaussian integration.

Time integration is performed using the Newmark method[7] with $\beta = 0.25$. The time step used in the numerical model is kept less than $0.5\,\mathrm{d}z/c$, where $\mathrm{d}z$ is the node spacing and c is the wave velocity. Since the pile has the highest wave velocity, the time step is calculated by taking $\mathrm{d}z$ and c of the pile.

In the elastic analyses, stresses at the pile–soil interface are obtained by the use of a stress smoothing technique given by Hinton and Campbell.[8] Here a patch of two soil elements is selected adjacent to the pile wall, and interface stresses are calculated at the mid-side soil node at the pile wall using stresses from the eight Gauss integration points of the soil element patch.

In the plastic analyses, the interface between pile and soil is modelled using a thin-layer interface element.[9,10] The stiffness of this element is calculated by assigning a width equivalent to one-tenth of the adjacent soil elements and using the same soil properties. Numerical integration is performed at two Gauss points on the centre line of the element. Mass of the interface element is neglected to avoid high natural frequencies present in elements with high stiffness and low mass.

When only displacements, axial stress in the pile and shear stresses are required, a coarser mesh is sufficient. The width of the element is selected by ensuring six nodes in the rising portion of the applied load, considering shear wave propagation across the soil plug. The height of the elements is selected by placing 12 nodes in the rising portion of the applied load, considering axial wave propagation in the pile. The validation of these criteria is presented in a later section.

Note that the aim of this model is not to represent a semi-infinite pile, but rather to remove the end effects from a pile with a plug of finite length.

DIMENSIONAL ANALYSIS

Before presenting results of the analysis, it is helpful to perform dimensional analysis, in order to identify the important dimensionless groups of relevant parameters. Dimensionless groups resulting from the input, deduced and output parameters are given in the Table I.

In order to illustrate the validity of these groups, three cases are analysed using the finite element method and keeping the input dimensionless groups constant. The parameters used for the analysis are given in Table II.

Pile radius and other geometric parameters used in Case 2 are obtained by reducing those used in Case 1 by a factor of two. To keep R^* constant, Z is kept in proportion to R^2 and m_r is kept in proportion to R^3. In Case 3, geometric parameters are identical to Case 1 but shaft friction is increased by a factor of two. Material properties of the pile and soil, and the hammer properties, are selected by keeping all dimensionless groups identical to those of Cases 1 and 2.

In the elastic analysis, shear and dilation wave transmitting boundaries are directly attached to the pile wall. Deeks[11] showed that a shear wave transmitting boundary alone is sufficient to represent the soil surrounding close-ended piles. For open-ended piles also, accurate results for pile displacement, axial stress in pile and shear stress inside the soil plug can be obtained by neglecting the dilation wave transmitting boundary. By including the dilation wave transmitting boundary, this model provides accurate radial, vertical and tangential stresses inside the soil plug. In the plastic analysis, soil surrounding the pile is extended to a distance equal to one half of the pile radius. This will be discussed in a later section.

Table I. Summary of parameters and dimensionless groups

Input parameters				Dimensionless
Hammer:	Ram mass		m_r	*
	Cushion stiffness		k_c	$k_c^* = k_c m_r / Z^2$
	Anvil mass		m_a	$m_a^* = m_a / m_r$
	Initial velocity of Ram		v_o	*
Pile:	Internal radius		R	$R^* = R / v_s t_r$
	Wall thickness		T	$T^* = T / R$
	Length		L	$L^* = L / R$
	Young's modulus		E_p	$E_p^* = E_p / \rho_p v_o^2$
	Density		ρ_p	$\rho_p^* = \rho_p A_p L / m_r$
	Poisson's ratio		v_p	v_p
Soil:	Height of plug		H	$H^* = H / R$
	Depth of penetration		H_o	$H_o^* = H_o / R$
	Poisson's ratio		v_s	v_s
	Density		ρ_s	$\rho_s^* = \rho_s / \rho_p$
	Shaft friction		f_s	$f_s^* = f_s v_s / G_s v_o$
	Shear modulus		G_s	$G_s^* = G_s / E_p$
Time:			t	$t^* = Z t / m_r$
Deduced parameters				
Cross-sectional area of pile		A_p	$2\pi(R + T/2)T$	A_p / A_o
Internal pile–soil area		A_o	$2\pi R H$	A_o / R^2
Cross-sectional area of soil plug		A_s	πR^2	A_s / A_o
Axial wave velocity of pile		c_p	$\sqrt{(E_p / \rho_p)}$	c_p / v_o
Shear wave velocity of soil		v_s	$\sqrt{(G_s / \rho_s)}$	v_s / v_o
Dilation wave velocity of soil		v_d	$\sqrt{(2G_s(1 - v_s)/\rho_s(1 - 2v_s))}$	v_d / v_o
Impedance of pile		Z	$A_p E_p / c_p$	*
Rise time		t_r		$t_r^* = Z t_r / m_r$
Output				
Displacement			u	$u^* = u / R$
Pile stress			σ_p	$\sigma_p^* = \sigma_p c_p / v_o E_p$
Soil Stresses:	Radial		σ_r	$\sigma_r^* = \sigma_r v_s / G_s v_o$
	Vertical		σ_z	$\sigma_z^* = \sigma_z v_s / G_s v_o$
	Shear		τ	$\tau^* = \tau v_s / G_s v_o$
	Tangential		σ_θ	$\sigma_\theta^* = \sigma_\theta v_s / G_s v_o$

Displacement of the pile obtained at the mid depth of soil plug from the elastic and plastic analyses for the three cases are shown in Figure 2. Identical dimensionless pile displacements show that, for a wide range of pile geometries, soil properties and hammer properties, identical dimensionless results can be obtained when the relevant dimensionless terms are kept constant.

ELASTIC RESPONSE OF SOIL PLUG TO HAMMER IMPACT

The response of open-ended piles to hammer impact mainly depends on the stress waves propagating inside the soil plug. The two types of stress waves propagating inside the soil plug can be identified as dilation waves and shear waves. To illustrate the general pattern of response, results will be presented initially for purely elastic conditions.

Table II. Values of parameters for three example analyses

	Case 1	Case 2	Case 3	Dimensionless
Properties of hammer				
m_r (kg)	10 000·0	1250·0	20 000·0	
m_a (kg)	5000·0	625·0	10 000·0	$m_a^* = 0{\cdot}5$
k_c (GN/m)	62·5	31·25	125·0	$k_c^* = 6{\cdot}25$
v_o (m/s)	5·0	5·0	5·0	
Properties of pile				
Z (MNs/m)	10·0	2·5	20·0	
R (m)	0·48	0·24	0·48	$R^* = 4.74$
L (m)	9·0	4·5	9·0	$L^* = 18{\cdot}75$
H (m)	8·0	4·0	8·0	$H^* = 16{\cdot}67$
A_p (m^2)	0·25	0·0625	0·25	
E_p (GN/m^2)	200·0	200·0	400·0	$E_p^* = 1 \times 10^6$
ρ_p (kg/m^3)	8000·0	8000·0	16 000·0	$\rho_p^* = 1{\cdot}8$
v_p	0·29	0·29	0·29	
Properties of soil				
f_s (KN/m^2)	115·0	115·0	230·0	$f_s^* = 0{\cdot}08$
v_s	0·45	0·45	0·45	
G_s (MN/m^2)	45·0	45·0	90·0	$G_s^* = 2.25 \times 10^{-4}$
ρ_s (kg/m^3)	2000·0	2000·0	4000·0	$\rho_s^* = 0{\cdot}25$

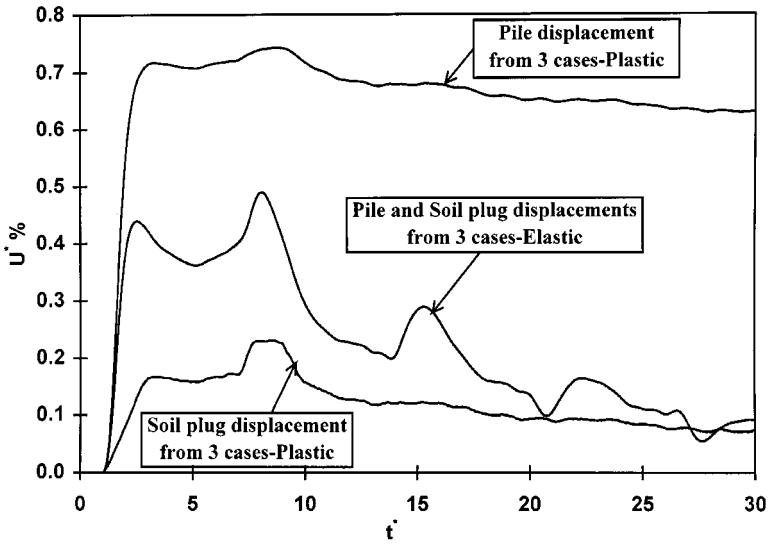

Figure 2. Displacements obtained from elastic and plastic analyses at mid-depth of soil plug

To obtain accurate results from the finite elements analysis, propagation of stress waves should be modelled accurately. Figure 3 shows shear stress, displacement and axial stress at the mid-depth of the pile obtained from a fine mesh and a coarse mesh, both including and neglecting radial degrees of freedom. Properties of the hammer–pile–soil system were those for Case 1 given

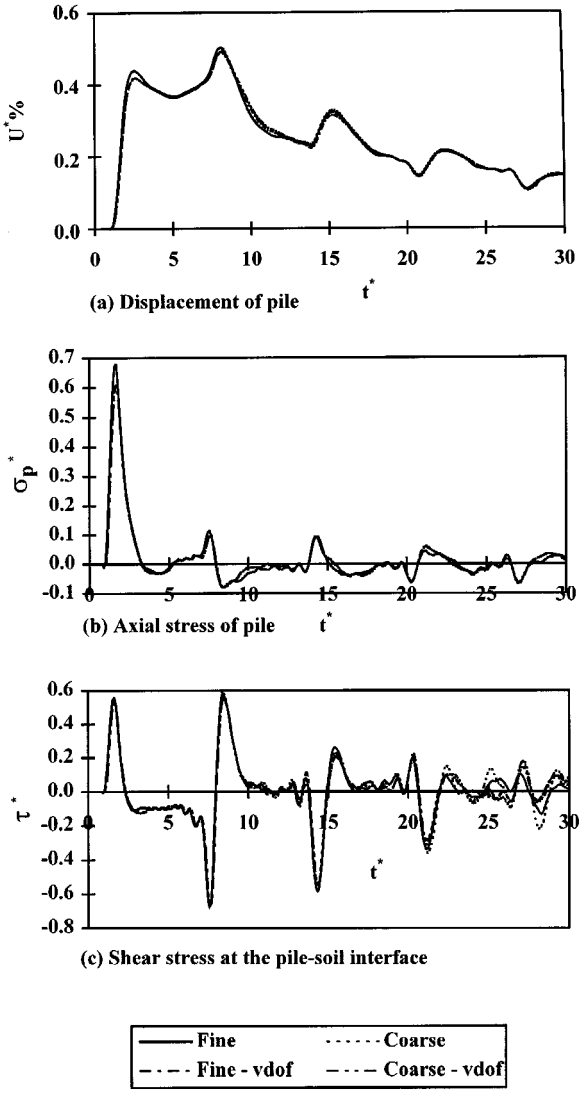

Figure 3. Effect of mesh fineness for elastic conditions (mid-depth of soil plug)

in Table 2. The element size for the coarse mesh was selected as described earlier. For the fine mesh, the width of the element was maintained the same as for the coarse mesh but, the height of the element was selected by ensuring six nodes in the rising portion of the applied load, considering the dilation wave propagation along the soil plug. For all four cases, the external soil field is truncated at a distance equal to the radius of the pile by applying transmitting boundaries.

For the cases with only vertical degrees of freedom and with both degrees of freedom, both fine and coarse meshes gave identical results. Therefore, for this problem, only propagation of radial shear and pile axial stress waves need to be modelled accurately.

Negative and positive peaks appearing in Figure 3(c) after the axial stress wave has travelled down the pile indicate that there is reversal in sign of the shear stress wave at the pile wall and when it passes through the centre. In Figure 4 propagation of the radial shear stress wave is shown at the mid-depth of the soil plug. The shear stress wave travelling inwards passes through the centre and travels towards the pile wall at the opposite end with changed sign. The shear stress wave reaching the pile wall is reflected with the same sign and thereafter the magnitude of the shear stress wave is reduced due to distructive interference of waves with opposite sign travelling across the soil plug. Randolph[12] postulated that the shear deformations may be assumed to die out by the central third of the pile shaft. However, according to finite element

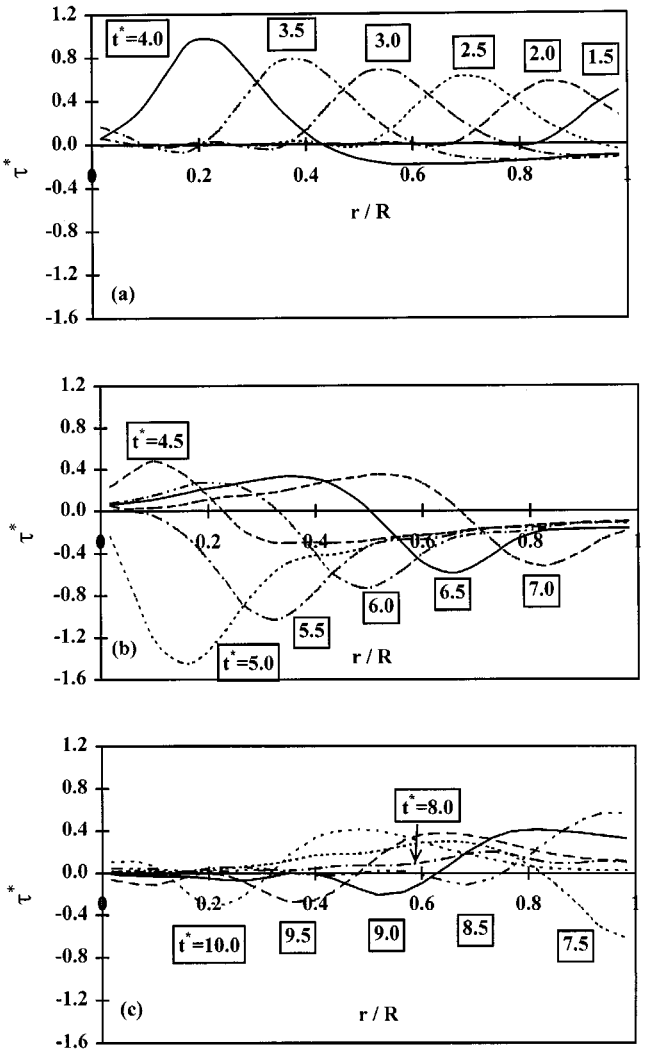

Figure 4. Shear stress wave propagation inside the soil plug (mid-depth of soil plug)

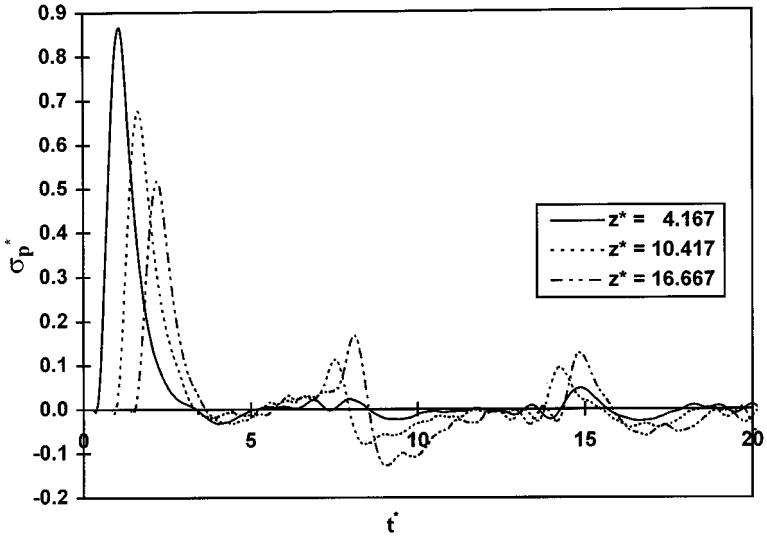

Figure 5. Variation of axial stress along the depth of the pile

analysis the magnitude of the stresses increases towards the centre line of the soil plug roughly in inverse proportion to $\sqrt{r}$.

The secondary peaks in Figure 3(b) indicate that a secondary axial stress wave is generated in the pile wall. The times at which these waves appear agree well with the times at which the peak value of the radial shear stress wave reflects at the pile wall. According to Figure 5, the effect of this secondary axial stress wave is more significant at lower levels of the soil plug (higher values of z^* where z^* is the non-dimensional depth z/R) than at the upper levels due to the addition of secondary waves travelling down the pile. However, the peak value of the applied impact load decays while travelling down the pile.

INELASTIC RESPONSE OF SOIL PLUG TO HAMMER IMPACT

The previous results for elastic conditions have illustrated the general pattern of stress wave propagation in the soil plug. Attention will now be turned to the more realistic situation where slip may occur between pile and soil. Inelastic response will be confined to the internal and external pile–soil interfaces only. Sliding between pile and soil is allowed to occur when the shear stress at the pile–soil interface reaches the limiting shaft friction. Finite element analysis is carried out using the initial stress method.[13] This method involves calculating the elastic displacement in each time step, then iterating to remove excess stresses.

The mode of pile penetration is determined by the displacement of the soil plug and external soil relative to the pile. In fully plugged piles the movement of the soil plug is equal to the movement of the pile. On the other hand, in completely unplugged piles the final movement of the soil plug is equal to the movement of the external soil. Based on field measurements Heerema and de Jong[14] stated that pipe piles generally penetrate in a partially plugged mode, where the plug advances up inside the pile more slowly than the pile penetrates past the external soil. The ratio of

the two movements has been referred to as the 'Incremental Filling Ratio' (IFR) by Brucy *et al.*[15] The tendency for the pile to plug, and hence the IFR, depends on the relative magnitude of the acceleration level, the mass of the soil plug, and the shaft friction.[16,17]

To select a suitable finite element mesh for the inelastic analysis, displacements obtained from six different finite element meshes were compared. In addition to the four meshes used in the elastic analysis, fine and coarse meshes with only vertical degrees of freedom were analysed by applying only a shear wave transmitting boundary directly to the pile wall. The results obtained at the mid-depth of soil plug for parameters given in Case 1 of Table 2 are shown in Figure 6. At

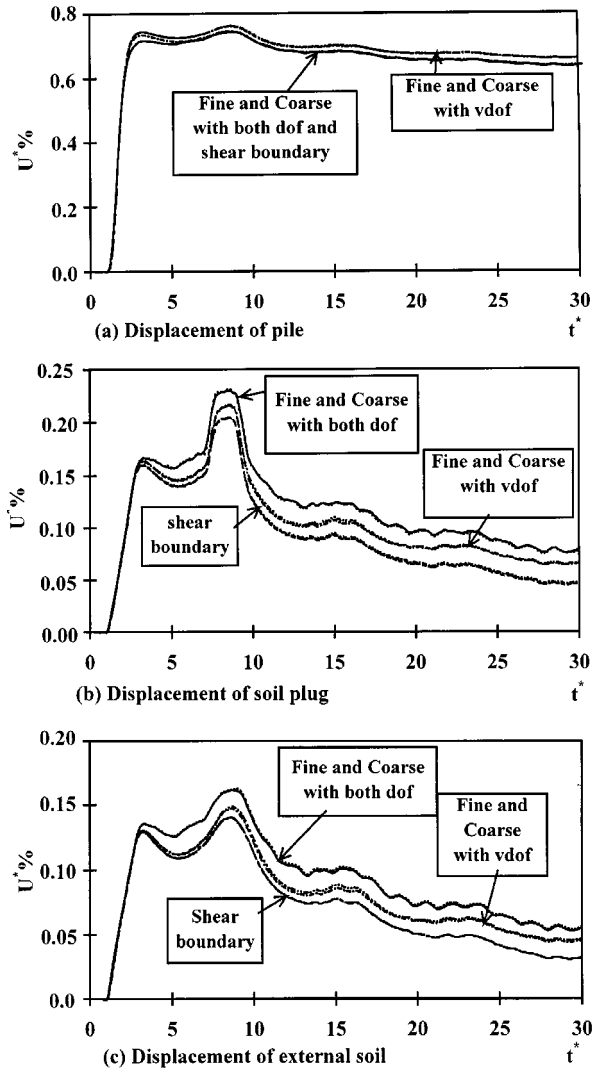

Figure 6. Effect of different meshes for plastic conditions (mid-depth of soil plug)

the end of the blow (for larger times than shown), the external soil movement reduces to essentially zero, while the displacement of the soil plug remains slightly positive.

The plastic movement between pile and soil plug measured at mid-depth of soil plug, expressed as a ratio of the final plastic pile displacement relative to the external soil, is 96, 97 and 98 percent, respectively, for the cases with both degrees of freedom, with only vertical degrees of freedom and with shear wave transmitting boundary directly attached to the pile. Clearly, results can be obtained to a reasonable level of accuracy when only vertical degrees of freedom are included by replacing the external soil field by the shear wave transmitting boundary. However, in what follows, a coarse mesh with both degrees of freedom has been used to present the results with high accuracy.

CONTRIBUTION OF SHAFT RESPONSE TO PLUGGING MECHANISM

Plugging of a pile alters its mode of penetration and affects the dynamic behaviour and static capacity of the pile. In the literature only limited attention has been paid to this phenomenon and its consequences. Currently, there is no reliable method to determine the penetration mode of open-ended piles prior to driving. By analysing field data, Paikowsky *et al.*[18] have proposed that there is a critical depth for pile plugging under conditions of standard dynamic driving. For the data analysed it appeared to be approximately equal to 75 times the pile diameter. Stevens[16] gave an expression for the plug length, up to which a pile should penetrate in terms of shaft friction, end bearing capacity, plug mass and plug acceleration. This expression was obtained by equating base resistance (based on gross area of pile) and the inertial resistance of the soil plug to shaft friction and weight of soil plug.

Here we consider the effect of $R^*(R/v_s t_r)$ and $f_s^*(f_s v_s/G_s v_o)$ on the mode of pile penetration. Since the analysis is performed for infinitely-long piles, results show only the contribution from the shaft to the mechanism of plugging. This is seen as an important first step before considering the additional complexity of interaction at the pile base.

A series of finite element analyses were performed by varying R^* for a particular value of f_s^*, while keeping other dimensionless terms constant. The dimensionless terms kept constant are identical to the values given in Table II, except for H^* and L^*. To obtain the height of the pile above soil $(L - H)$ equal to one element height for the case with smallest R^*, H^* and L^* are increased to 50·0 and 62·5. In the finite element model, the external soil field was truncated by applying shear and dilation wave transmitting boundaries at a distance equal to the radius of the pile. The IFR was calculated as the gradient of the graph of penetration depth versus height of soil column[15]. This is similar to the definition of 'specific recovery ratio' given by Paikowsky and Whitman.[19] For fully plugged piles IFR = 0 percent and for completely unplugged piles IFR = 100 percent. Since the geometries of the finite element models are different, IFR is calculated at the mid-depth of the soil plug, after the first reflection of the radial shear stress wave at the pile wall has occurred.

According to Figure 7, the IFR increases with R^*, and decreases with f_s^*. The change in IFR becomes negligible once R^* is greater than 4. From the shape of the applied impact load, the load becomes negligibly small (less than 1·5 per cent of the peak value) for times greater than four times t_r. Hence, when R^* is greater than 4, there is no interaction between the incident and reflected waves, and the response therefore becomes independent of R^*.

Negative values of IFR were observed when the final displacement of the soil plug was greater than that of the pile. In these cases no yielding occurred at the first positive peak shear stress.

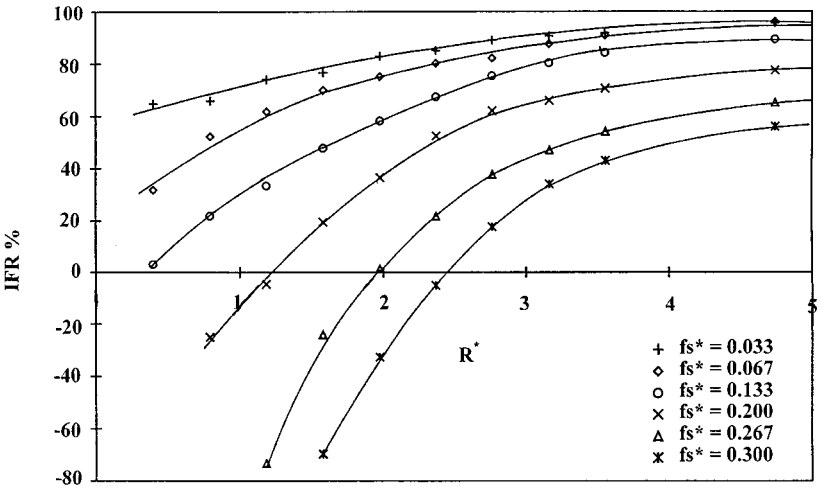

Figure 7. Variation of IFR with R^* and f_s^*

Yielding first occurred at the first negative peak shear stress and the soil plug slipped in the opposite direction. In reality, however, the final displacement of the soil plug cannot exceed that of the pile during steady state driving. In practice, residual stresses will build up in the soil plug, originating from the pile base, such that the IFR value will become zero.

From the above analysis it is clear that the radius of the pile, the shape of the applied impact load and the shaft friction have great influence on the penetration mode of the pile.

ONE-DIMENSIONAL MODELLING OF THE PILE AND SOIL

One-dimensional modelling of the pile shaft requires appropriate soil models to represent the load transfer along the inside and the outside walls of the pile. Since the introduction of wave equation analysis by Smith,[20] considerable research effort has been expended in the modelling of the soil reaction along the pile shaft and at the pile base. The soil model proposed by Smith[20] consisted of a spring and slider in parallel with a viscous dashpot. When applying this model for open-ended piles, prior to an analysis, the status of the soil plug (whether plugged or unplugged) has to be assumed. If it is unplugged, additional resistance is lumped onto the shaft. This model cannot distinguish between the inner and outer shaft friction.

Heerema and de Jong[14] modelled the soil plug as a mass–spring system inside the mass–spring system of the pile, with frictional forces acting between the soil nodes and pile nodes. Viscous dampers are included between each soil plug node to reduce the oscillations of soil column. External shaft friction is modelled in a similar manner to Smith.[20]

Randolph and Simons[21] also used the same 'pile-in-pile' approach to model the soil plug, but the external soil model was based on Novak's[22] solution. This solution idealizes the soil as a series of independent horizontal layers. The shear force mobilized per unit length of external pile shaft is taken as $T = K_s U + C_s(\mathrm{d}U/\mathrm{d}t)$, where $K_s = 2{\cdot}9G_s$, $C_s = 2\pi R_o(G_s\rho_s)^{1/2}$ and R_o is the external pile radius. The important difference in this model compared to the above two models is that the external shaft friction is given in terms of fundamental soil properties.

Randolph[12] improved the above model by inserting a soil model identical to the external soil model between the pile wall and central soil mass as detailed in Figure 9. The basis of this model is that, close to the pile, the dynamic response of internal and external soil is likely to be the same. The spring part of the inner soil model was assigned $5{\cdot}8G_s$, which is twice the outer value, on the assumption that shearing was confined to the outer part of the soil plug only. The shear force mobilized per unit length of inner pile shaft was taken as $T = K_i U + C_i(\mathrm{d}U/\mathrm{d}t)$, where $K_i = 5{\cdot}8G_s$, $C_i = 2\pi R_i(G_s\rho_s)^{1/2}$ and R_i is the inner pile radius.

The above one-dimensional models do not consider the effect of propagation of the shear stress wave in the radial direction of the soil plug as discussed in the previous sections. Shear stress mobilization at the internal and external walls is modelled in a similar manner. By using the finite

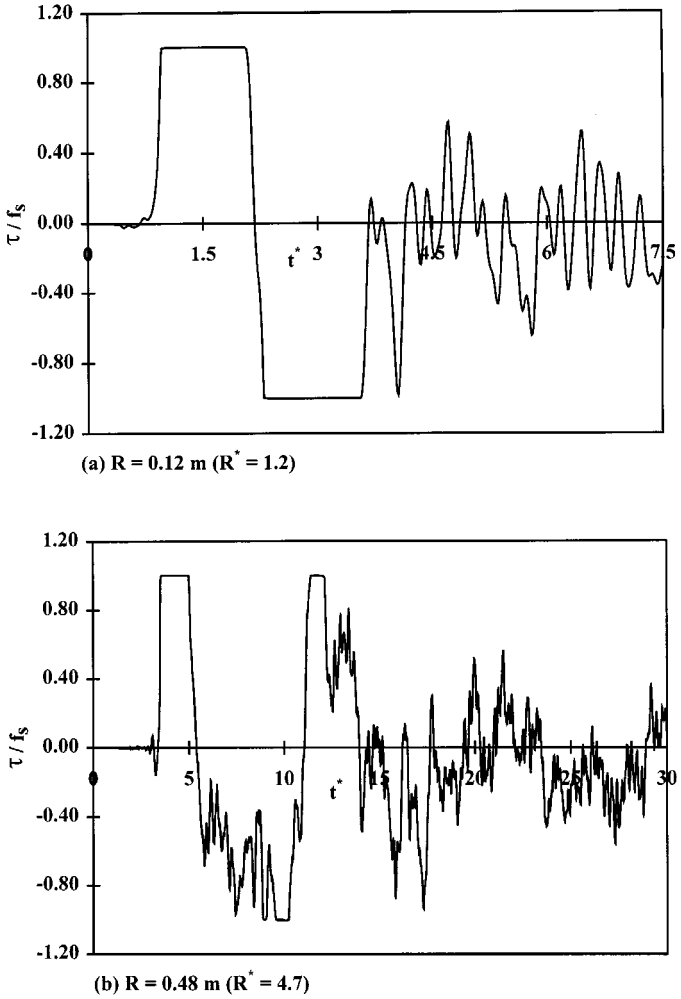

Figure 8. Shear stress obtained at internal pile–soil interface (mid-depth of soil plug) by limiting f_s to 100 kPa ($f_s^* = 0{\cdot}067$)

element method, the soil plug response can be obtained accurately, provided that a fine mesh and a small time step are used; but this is time consuming and expensive.

Earlier it was shown that the response of the shaft obtained by considering only vertical degrees of freedom for the soil plug, and by applying a shear wave transmitting boundary at the external wall of the pile, agreed reasonably well with the finite element results. Hence, it is adequate to include only vertical degrees of freedom in the simplified one-dimensional model. External shaft response can be obtained by using the shear wave transmitting boundary detailed above.

For the soil plug response, a frequency-independent analytical solution cannot be obtained. It was found that the soil plug slips only up to the time the radial shear stress wave reflected at the centre for the first time reaches pile wall, even if the shaft friction is reduced to less than only the lowest of the first three or first four positive or negative peaks. This appears to be true irrespective of the normalized pile radius, R^*. The shear stresses obtained from the finite element analysis for the two cases with $R^* = 1{\cdot}2$ and $R^* = 4{\cdot}7$ are given in Figure 8. Therefore, in the one-dimensional model it is adequate to represent only the first two positive and first negative peak shear stresses.

For the analysis which follows, a one-dimensional model consisting of spring and dashpot, similar to the one given in the IMPACT program[23] is used. The spring constant used for the external shaft is equal to πG_s and the dashpot constant is $2\pi R_o(G_s\rho_s)^{1/2}$, as recommended by Deeks and Randolph.[5] Results given in Figure 6 show that, by applying this model to represent the external soil, results can be obtained with reasonable accuracy.

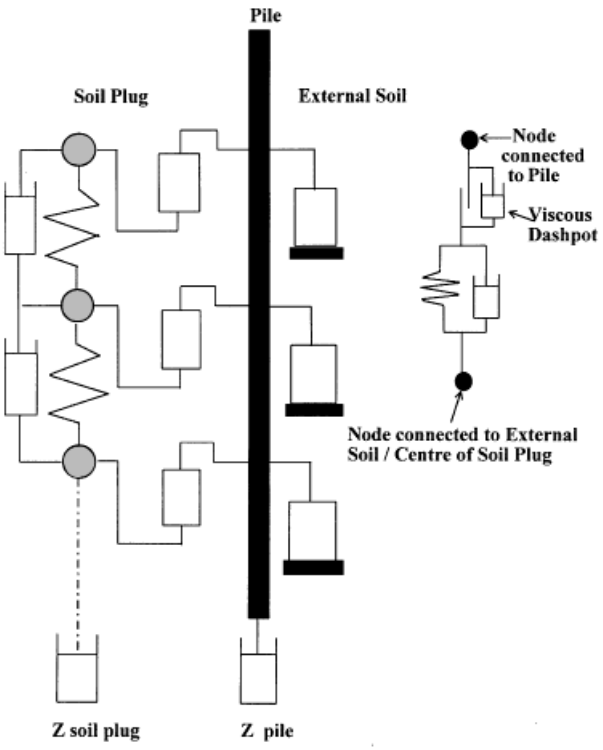

Figure 9. One-dimensional model

The IMPACT model uses $5{\cdot}8G_s$ for the inner shaft springs. This high stiffness was based on an assumption which has now been shown to be incorrect. Outside the pile, waves geometrically attenuate while travelling away from the pile. Inside the soil plug, waves are geometrically amplified while travelling towards the centre. However, at the inner and outer pile–soil interfaces, the situations should be similar until the waves pass from one side of the pile to the other. Therefore in the model used here, an internal spring constant of πG_s is used.

The pile is modelled using two-node tube elements with consistent mass, and the soil plug is modelled using two-node rod elements with lumped mass. Viscous dashpots are incorporated in parallel with the axial springs representing the soil plug as shown in Figure 9, similar to the

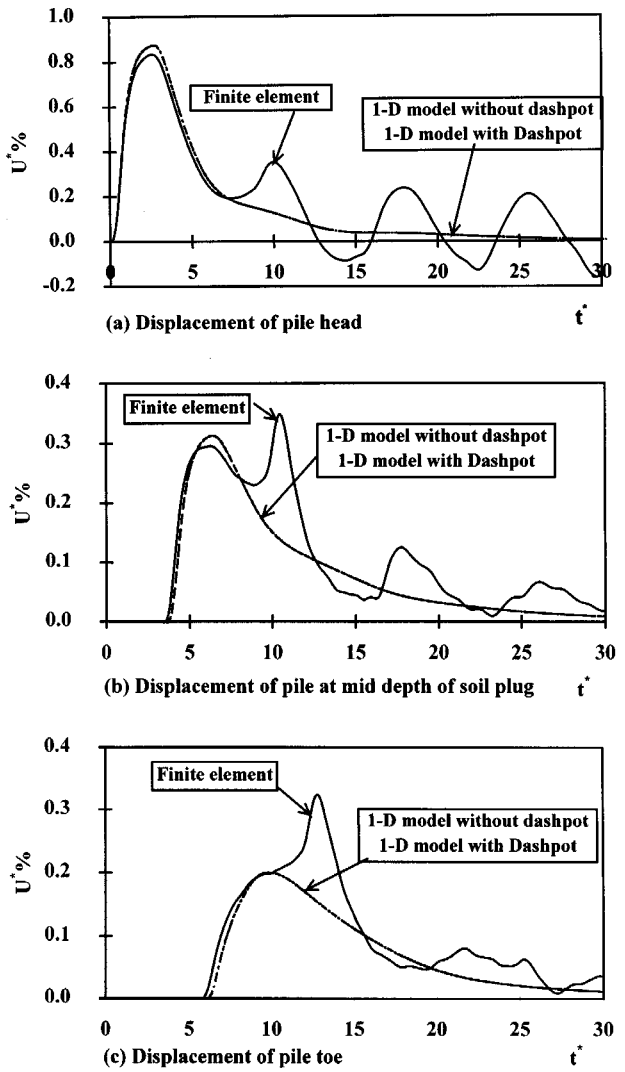

Figure 10. Comparison of displacements for elastic conditions ($R^* = 4{\cdot}7$)

IMPACT model. The damping coefficient is calculated based on the cross-sectional area of the soil plug, ρ_s and the dilation wave velocity of soil. To simulate the conditions of an infinitely-long pile, dashpots equivalent to the impedances of the pile and soil plug are attached to the pile toe and to the bottom of the soil plug, respectively.

The equation of motion of this model is

$$f(t) = K(u) + C(\mathrm{d}u/\mathrm{d}t) + M(\mathrm{d}^2u/\mathrm{d}t^2)$$

where K is the stiffness matrix, C is the damping matrix, M is the mass matrix and $f(t)$ is the force exerted on the pile. Time integration of the above equation was carried out in a similar manner to the finite element analysis. Distance between nodes was selected by placing twelve nodes in the rising portion of the applied force according to the axial wave velocity in pile. This is equal to the node spacing used in the finite element analysis in the vertical direction.

COMPARISON OF ONE-DIMENSIONAL AND FINITE ELEMENT RESULTS

Figures 10–12 show results obtained for $R^* = 4{\cdot}7$. Since wave propagation in the radial direction is not allowed in the pile-in-pile model, only the stresses corresponding to first peak are modelled with any accuracy. Shear stress, displacement and axial stress corresponding to the first peak agrees well with those obtained from the finite element analysis. However, this would not be the same for all values of R^*. When R^* is less than one, the first peak axial stress is modified by the shear stress wave reflected at the pile wall. Therefore, the first peak axial stress given by the pile-in-pile model should be lower than that obtained from the finite element analysis, and this results in lower shear stress and displacement at the first peak.

Identical results were obtained with and without the viscous dashpots attached to the soil plug parallel to the axial springs. It can be concluded that there is no stress wave of significant magnitude travelling along the central soil column in the vertical direction when only the shaft response is considered.

Figure 13 shows displacements obtained from the inelastic analysis for $R^* = 4{\cdot}7$. In the pile-in-pile model results were obtained by modelling the pile–soil interface using a rigid-plastic

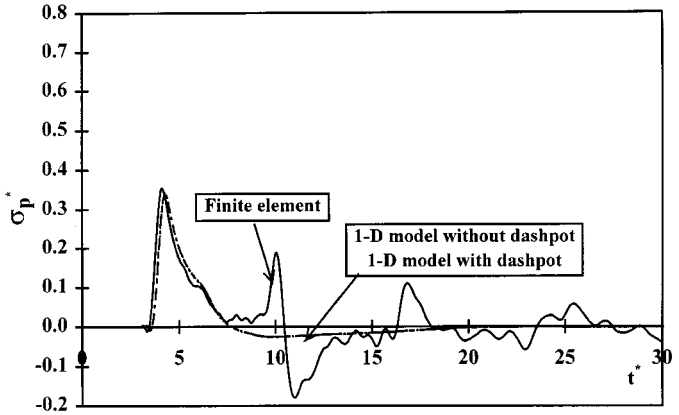

Figure 11. Comparison of axial stresses for elastic conditions at mid depth of soil plug ($R^* = 4{\cdot}7$)

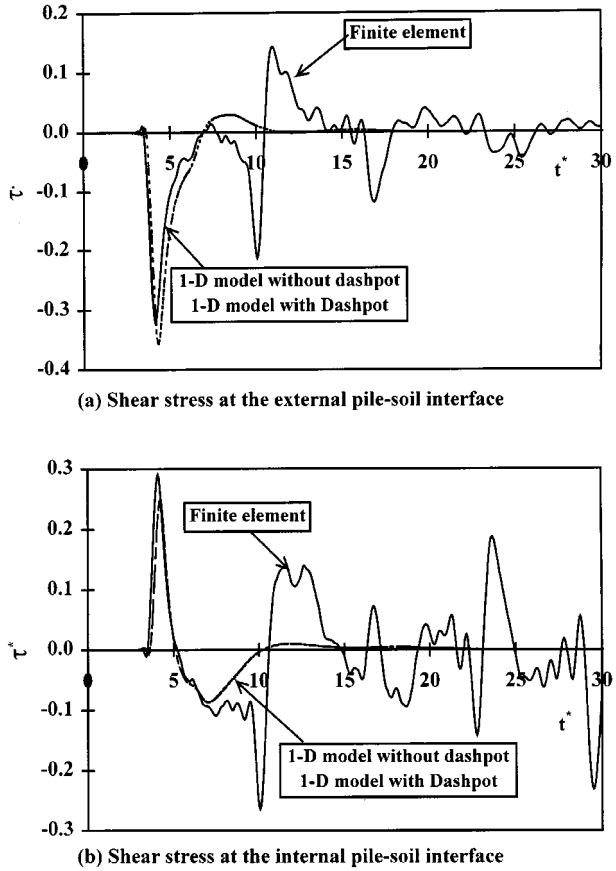

Figure 12. Comparison of shear stresses for elastic conditions at mid-depth of soil plug ($R^* = 4{\cdot}7$)

slider. Displacement of the pile obtained from the finite element method and the pile-in-pile model agrees well. For displacement of the soil plug adjacent to pile, and external soil adjacent to the pile, good agreement can be observed after the second slip, which indicates that the agreement between total slip in the finite element and pile-in-pile models is good.

Figure 14 shows finite element and lumped mass model results obtained for $R^* = 2{\cdot}0$ and $f_s^* = 0{\cdot}267$ from inelastic analysis. These conditions correspond to fully plugged response of the soil plug. In the lumped-mass model external soil is modelled similarly to the pile-in-pile model. However, in the lumped-mass model slip is not allowed to occur between soil plug and pile since the intention is to simulate 'plugged' response, with IFR = 0 percent. It may be seen that there is good agreement between the displacements obtained for the two cases shown in Figure 14.

APPLICABILITY OF ONE-DIMENSIONAL MODELS TO THE PILE DRIVING PROBLEM

In open ended piles, accurate representation of soil displacements is important in order to determine the penetration mode. Figure 15 shows the percentage difference in IFR obtained from

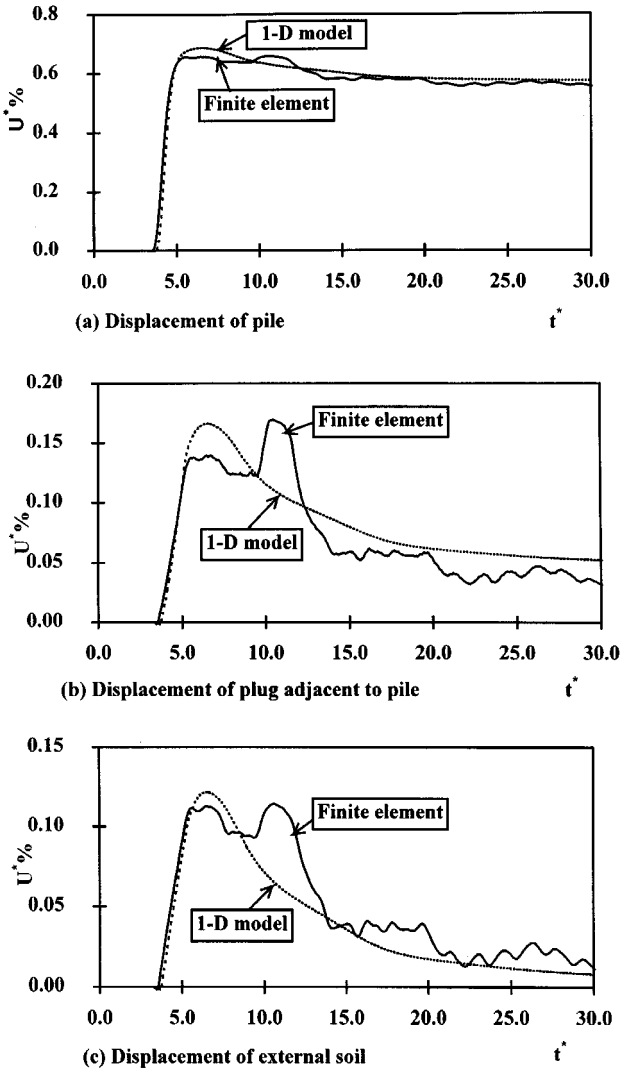

Figure 13. Comparison of displacements for plastic conditions at mid-depth of soil plug ($R^* = 4{\cdot}7$)

the comparison of results from the one-dimensional models and the finite element method. Clearly, the performance of the pile-in-pile model is not the same for all values of R^* and f_s^*. Dotted lines in Figure 15 show the percentage error contour lines. Along any contour line both f_s^* and R^* vary. When R^* and f_s^* lie above any curved-contour line, results can be obtained with an error less than that of the relevant contour line from the pile-in-pile model.

When the soil plug movement is small (IFR ~ 0 percent), analysis can be carried out by lumping the mass of inner soil column to the pile wall. The shaded area with two horizontal boundaries given in Figure 15 shows the region within which results can be obtained using this model with an

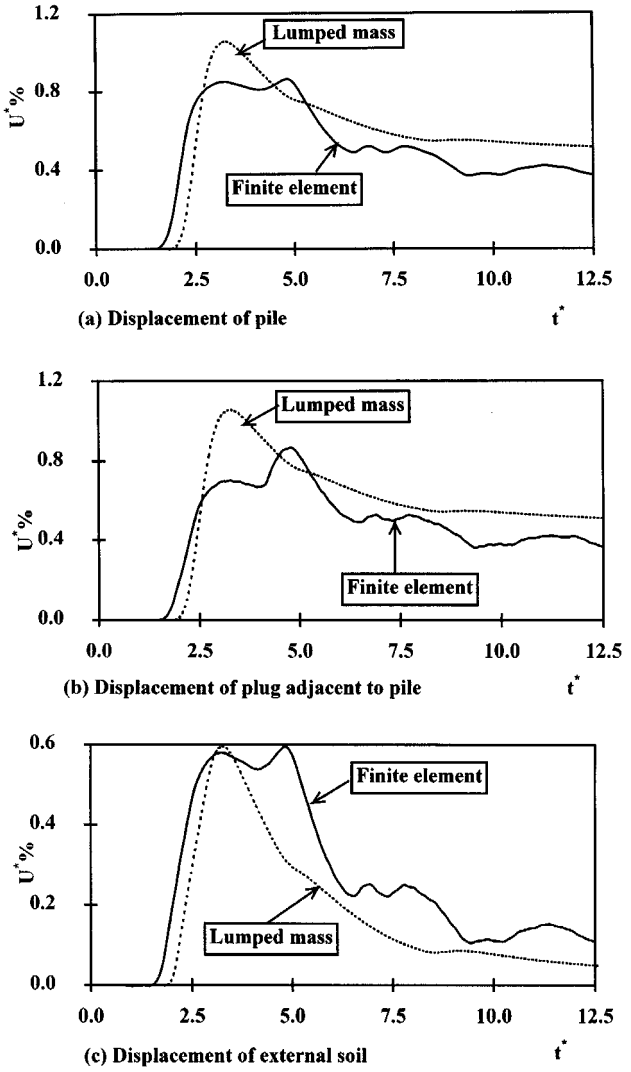

Figure 14. Comparison of displacements for plastic conditions at mid-depth of soil plug ($R^* = 2{\cdot}0$, $f_s^* = 0{\cdot}267$)

accuracy of $\pm$ 10·0 per cent difference. For values of f_s^* and R^* which do not lie within the two shaded regions, where both lumped-mass and pile-in-pile model give results with difference greater than 10·0 percent, finite element analysis should be used. In the finite element model, only vertical degrees of freedom need be included, and the external soil can be replaced by the shear wave transmitting boundary, as shown earlier. Using a chart like Figure 15, the penetration mode of a pile can be obtained prior to driving if R^* and f_s^* are known. In addition the chart shows the type of simplified model that can be used for analysis of the pile driving process to obtain accurate results.

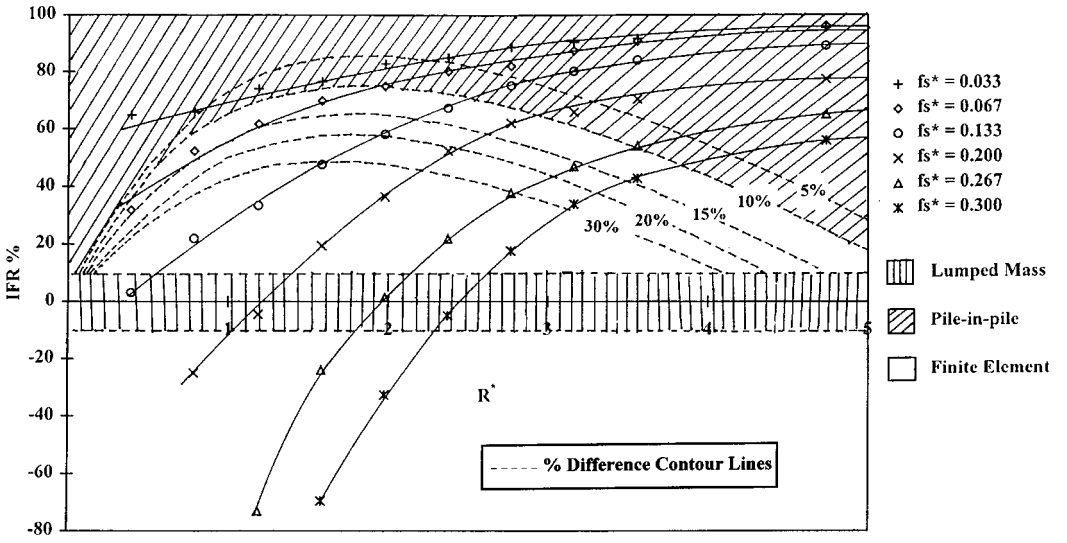

Figure 15. Comparison of results obtained from the finite element and one-dimensional models

CONCLUSIONS

The main intent of this study was to examine the parameters affecting the plugging mechanism of open-ended piles and to investigate the use of simplified models to analyse the driving process of open-ended piles.

First a dimensional analysis was carried out. It was shown that by keeping the dimensionless groups constant, identical dimensionless results can be obtained for different pile geometries and soil properties.

By observing the stress wave propagation inside the soil plug, the primary wave propagating in the soil plug was shown to be the shear stress wave travelling in the radial direction. As a result of this wave a secondary axial stress wave is generated.

Finite element analysis was carried out for several values of non-dimensionalised pile radius (R^*) and internal shift friction (f_s^*) , by keeping all other dimensionless terms constant. When only shaft response is considered, the penetration mode of a pile mainly depends on the friction at the pile–soil interface, the shear wave velocity of the soil and the shape of the applied load. If the first negative peak of the internal shear stress exceeds the limiting shaft friction instead of the first positive peak shear stress, the displacement of the soil plug exceeds that of the pile. Due to base resistance, this is unlikely to occur in reality; instead, compaction of the bottom layers of the soil plug may occur.

One-dimensional models found in the literature were discussed, and it was shown that for a particular range of R^* and f_s^* internal shaft friction can be modelled using a spring, dashpot and a slider identical to the external shaft friction. To analyse piles with near zero IFR, the soil plug mass can be lumped to the pile wall. For the range of R^* and f_s^* in which neither model gives accurate results, the soil plug can be modelled using eight-node rectangular elements with only vertical degrees of freedom. Node spacing in the vertical direction can be selected by considering wave velocity in the pile. This allows a coarse

mesh to be used, and consequently the number of equations which must be solved is reasonably small.

REFERENCE

1. Y. K. Chow, 'A numerical model for the analysis of pile driveability.', *Proc. 2nd Int. Conf. on the Application of Stress Wave Theory on Piles*, May 1984, pp. 27–30.
2. H. A. Simons, A Theoretical Study of Pile Driving, *Ph.D. Thesis*, University of Cambridge, 1985.
3. I. M. Smith, P. To and S. M. Wilson, 'Plugging of pipe piles.' *3rd Int. Conf. on Numerical Methods in Offshore Piling*., Nantes, 1986, pp. 53–73.
4. O. G. Ugaz, An Experimental and Numerical study of Impact Driving of Open-ended Pipe Piles in Dense Saturated Sand, *Ph.D. Thesis*, University of Houstan, 1988.
5. A. J. Deeks and M. F. Randolph, 'Axisymmetric time-domain transmitting boundaries', *J. Engng. Mech.* ASCE, **120,** 25–41 (1994).
6. A. J. Deeks and M. F. Randolph, 'Analytical modelling of hammer impact for pile driving'. *Int. J. Numer. Anal. Meth. Geomech*., **17,** 279–302 (1993).
7. K. J. Bathe and E. L. Wilson, *Numerical Methods in Finite Element Analysis*, Prentice-Hall, Englewood Cliffs NJ, 1976.
8. E. Hinton and J. S. Campbell, 'Local and Global smoothing of discontinuous finite element functions using a least squares method.' *Int. J. Numer. Meth. Engng*. **8,** 461–480 (1974).
9. O. C. Zienkiewicz, B. Best, C. Dullage and K. G. Stagg, 'Analysis of nonlinear problems in rock mechanics with particular reference to jointed rock systems.' *Proc. 2nd Int. Conf. Soc. of Rock Mech*., Belgrade, **3** (1970) pp. 501–509.
10. C. S. Desai, M. M. Zaman, J. G. Lightner and H. J. Siriwardena, 'Thin-layer element for interfaces and joints.' *Int. J. Numer. Anal. Meth. Geomech*., **8,** 19–43 (1984).
11. A. J. Deeks, Numerical Analysis of Pile Driving Dynamics, *Ph.D. Thesis*., University of Western Australia, 1992.
12. M. F. Randolph, 'Modelling of the soil plug response during pile driving.' *Proc. 9th S. E. Asian Geotechnical Conf*., Bangkok, **2,** 1987, pp. 6.1–6.14.
13. I. M. Smith and D. V. Griffiths, *Programming the Finite Element Method*. Wiley, New York, 1988.
14. E. P. Heerema and A. de Jong 'An advanced wave equation computer program which simulates dynamic pile plugging through a coupled mass-spring system.' *Proc. Int. Conf. on Numerical Methods in Offshore Piling*, ICE, London, (1979) pp. 37–42.
15. F. Brucy, J. Meunier and J. F. Nauroy, 'Comparison of static and dynamic tests of piles in sand.', *Int. Conf. on Deep Foundations*, Paris, March 1991.
16. R. F. Stevens, 'The effect of a soil plug on pile drivability in clay' *3rd Int. Conf. on Application of Stress Wave Theory to Piles*, Ottawa, Canada (1988) pp. 861–868.
17. F. Brucy, J. Meunier and J. F. Nauroy, 'Behaviour of pile plug in sandy soils during and after driving.', *Proc. 23rd Offshore Technology Conf*., May 1991, pp. 145–154.
18. S. G. Paikowsky, R. V. Whitman and M. M. Baligh, 'A new look at the phenomenon of offshore pile plugging.' *Marine Geotech*., **8,** 213–230 (1990).
19. S. G. Paikowsky and R. V. Whitman, 'The effects of plugging on pile performance and design.' *Can. Geotech. J*., **27,** 429–440 (1990).
20. E. A. L. Smith, 'Pile driving analysis by the wave equation.' *J. Soil Mech. Found. Engng. Div*., ASCE, **86,** 35–61 (1960).
21. M. F. Randolph and H. A. Simons, 'An improved soil model for one-dimensional pile driving analysis'. *3rd Int. Conf. on Numerical Methods in Offshore Piling*, Nantes, (1986), pp. 3–18.
22. M. Novak, 'Vertical vibration of floating piles' *J. Engng. Mech. Div*., ASCE, **103,** 153–168 (1977).
23. M. F. Randolph, *IMPACT Program Manual*, The university of Western Australia, 1992.

